Friction https://mc03.manuscriptcentral.com/friction
https://doi.org/10.26599/FRICT.2026.9441264

Research Article

The effect of group 5 metal elements addition to ta-C coating on tribological properties in dry friction

Takayuki Tokoroyama[1*], Kosuke Suzuki[1], Asato Tanigawa[1], Ruixi Zhang[1], Lulu Li[1], Noritsugu Umehara[1], Jongkuk Kim[2], Jae-Il Kim[2], Young-Jun Jang[2,4], Motoyuki Murashima[3]

[1]*Department of Micro-Nano Mechanical Science and Engineering, Graduate School of Engineering, Nagoya University, Furo-cho, Chikusa-ku, Nagoya, Aichi 464-8603, Japan*

[2]*Department of Extreme Environmental Coatings, Korea Institute of Materials Science, 797, Changwon-daero, Seongsan-gu, Changwon-si, Gyeongsangnam-do, 51508, Republic of Korea*

[3]*Department of Mechanical Systems Engineering, Graduate School of Engineering, Tohoku University, 6-6-01 Aramaki-aza-aoba, Aoba-ku, Sendai 980-8579, Japan*

[4] *Department of Aerospace Materials Engineering, University of Science and Technology (UST), 217 Gajeong-ro, Yuseong-gu, Daejeon 34113, Republic of Korea*

* Corresponding author: Takayuki Tokoroyama, E-mail: takayuki.tokoroyama@mae.nagoya-u.ac.jp

Received: July 20, 2025; Revised: March 26, 2026; Accepted: May 7, 2026

Abstract: Carbon-based hard coatings are ideal for mechanical materials due to their high hardness. However, maintaining low friction in air requires suppressing oxidation by atmospheric oxygen to protect the graphite structure, known for its low friction properties. This study introduced Group 5 elements (vanadium, niobium, tantalum) into the coatings to safeguard the graphite structure and enhance wear resistance through oxidation and reduction reactions. Using an ta-C coating with a high sp^3 carbon structure, the effects of these elements were analyzed. The ta-C:Ta coating, containing tantalum, achieved the lowest average friction coefficient of 0.043 in air, followed by ta-C:Nb at 0.067, demonstrating the potential of Group 5 elements to improve coating performance.

Keywords: 5 metal elements; ta-C; friction; Raman; XPS

1 Introduction

Materials with low friction in the atmosphere are highly attractive. Substances with a layered sliding mechanism within the contact surface, such as solid lubricants, are important low-friction materials in environments where lubricating oil cannot be used. However, since layered structure materials generate low friction by causing cleavage sliding under shear force, if they are discharged from the contact surface, they can no longer maintain low friction. From this perspective, graphite and molybdenum disulfide (MoS_2), commonly used as low-friction materials in atmospheric conditions, have low wear resistance and are not considered long-lasting materials. Therefore, carbon-based hard thin coatings are expected to be one potential candidate material. Carbon-based hard thin coatings are materials that are expected to exhibit not only high hardness but also low friction [1, 2]. The DLC coatings can be broadly classified into hydrogen-containing [3–7], non-hydrogen-containing [8-13], and other element-doped types [14–18]. It has also been reported that in friction within lubricating oil, differences such as the ease of tribofilm formation due to the structure within the coating can affect friction characteristics [19–26]. However, it is difficult to achieve a low coefficient of friction below

0.1 in the atmosphere. Surface treatment methods to reduce the friction coefficient are also being studied [27–30]. For carbon-based hard thin coatings to exhibit low friction in the atmosphere as solid lubricating materials, it is believed that either the entire coating must be rich in sp^3 structure and hard, while the topmost surface (the contact surface) must possess an sp^2 structure with low shear resistance, or the topmost surface must contain numerous fragments of graphite structures, where the hexagonal ring structure of graphite formed by carbon atoms becomes incommensurate, meaning it does not align with the sliding direction [31, 32]. The cause of not achieving a low friction coefficient in the atmosphere is speculated to be either the removal of the low shear resistance layer due to friction, or the graphite structure being oxidized or disrupted by the adsorption of oxygen or moisture from the atmosphere [33, 34].

In the future, for carbon-based hard thin coatings to be used as low-friction materials in atmospheric conditions, it will be essential to maintain the graphite structure of the topmost surface without oxidation, despite the presence of oxygen and moisture from the environment. The authors have previously conducted research aiming to achieve high-temperature stability by introducing silicon (Si) into tetrahedral amorphous carbon (ta-C) coatings [35]. It was revealed that by incorporating Si into ta-C coatings, the I_D/I_G ratio within the coating structure remains unchanged even after heating up to 400°C, and the hardness can be maintained at approximately 30 GPa. However, achieving a low friction coefficient of 0.1 or less proved to be challenging. Although Si-DLC (a-C:H:Si) can exhibit a friction coefficient nearly equal to 0.05 in air with a hardness of around 20 GPa. Its tribological performance strongly depends on the hydrogen-containing Si-oxide formation, which lacks thermal stability above ~350°C [36]. In contrast, ta-C:Ta and ta-C:Nb form thermally stable TaOx and NbOx phases while maintaining a hydrogen-free carbon matrix. This leads to significantly higher wear resistance and improved high-temperature durability compared to Si-DLC. In this study, we investigated a method of introducing group 5 elements into the coating to improve its oxidation resistance. Group 5 elements, arranged in order of atomic radius, include vanadium (V), niobium (Nb),

and tantalum (Ta), all of which form oxides. Among them, it has been reported through first-principles calculations that when carbon is included as an impurity in the Ta_2O_5 crystal structure, the Ta-O bond energy decreases, making oxygen more likely to desorb [37]. If the oxidation and oxygen desorption of group 5 metal elements within the carbon atom framework of the hard thin coating can suppress the oxidation of nearby carbon atoms, there is potential to maintain low friction in atmospheric conditions. The authors have previously conducted experiments to achieve a low friction coefficient by incorporating group 5 elements into a-C coatings which was very close hardness as ta-C around 30 GPa. To further clarify the mechanism behind the manifestation of low friction, they are focusing on the same group 5 elements in this study. [38–40].

From the above perspective, vanadium, niobium, and tantalum were introduced into tetrahedral amorphous carbon (ta-C) coatings, which are high-hardness carbon thin coatings, using the arc deposition for carbon and sputtering method for elements. The friction and wear properties in atmospheric and oxygen environments were evaluated. Additionally, the mechanical properties of the obtained coatings, the measurement of their heat resistance temperature, and the impact of the oxygen concentration in the coatings before and after friction on their frictional properties were clarified.

2 Experimental procedure

2.1 Preparation of ta-C coating with 5 metal elements via IBA-FAD method

A schematic diagram of the deposition apparatus used in this study is shown in Fig. 1 [41]. The deposition method is a physical vapor deposition process using arc discharge on a carbon target, with almost no hydrogen included in the coating. Carbon atoms and ions evaporated from the carbon target travel straight through the piping, and only the carbon ions are bent 90 degrees by the electromagnet installed in the pipe, being introduced into the deposition chamber. The base pressure before deposition was 4.0×10^{-4} Pa. To clean the surface of the carbon target and the inside of the piping, pre-arc discharge was performed for 20 minutes at a current of 40 A and a duct bias voltage of 15 V. It is

possible to obtain coating hardness higher than 30 GPa as ta-C via the equipment. Tungsten carbide (φ22.5 mm, thickness 4 mm) was used as the deposition substrate, and before deposition, ultrasonic cleaning was performed in benzine (15 minutes) followed by acetone (15 minutes). The test piece was fixed to a rotating substrate stage installed inside the deposition chamber, and Ar sputter cleaning was conducted for 20 minutes (Ar flow rate: 16 sccm, discharge voltage: 1.8 kV, substrate rotation speed: 4 rpm). Using the magnetron sputtering method, sputtering was performed on five metal elements, and deposition was carried out so that they were incorporated into the ta-C coating. A discharge current of 300 mA was used for each target.

The results of the coating hardness and surface roughness after deposition, nano-indentation hardness (Elionix; ENT1100-a, Berkovich type diamond tip), and surface roughness measurement (measured by using AFM (Shimazu; SPM-9700HT)) are shown in Table 1. The hardness of the coating remained almost unchanged when V was incorporated compared to the ta-C coating, but it decreased when Nb and Ta were incorporated. The slight decrease in the Young's modulus of ta-C:V compared with ta-C, despite similar hardness, was attributed to the partial formation of V-C bonds and to the presence of vanadium atoms that locally disturb the continuous covalent carbon network. These effects relax local stress and reduce elastic recovery while maintaining overall hardness. Similarly, when Nb and Ta are incorporated into the ta-C matrix, the formation of new bonds or the presence of metal atoms within the carbon network is considered to induce partial discontinuities in the network structure, leading to a decrease in hardness. Although the hardness of Me-doped coatings decreases due to the introduction of metallic bonding, the carbon matrix retains a high sp^3 fraction characteristic of ta-C which is shown in section 3.3. Therefore, the doped coatings are referred to as ta-C:Me in accordance with their structural signature rather than hardness alone.

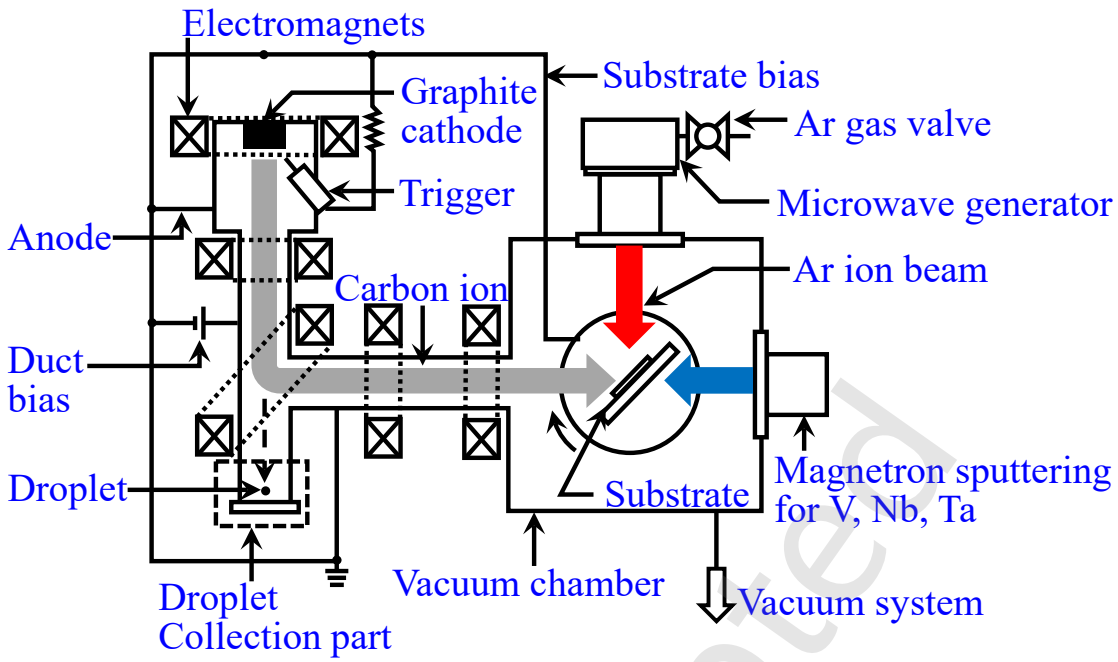

Fig. 1 Schematic illustration of the IBA-FAB with a magnetron sputtering of metal element equipment.

Table 1 Mechanical properties of each coating.

	ta-C	ta-C:V	ta-C:Nb	ta-C:Ta
Coating thickness *t*, nm	496	330	360	322
Arithmetic-average surface roughness *Ra*, nm	7.1	6.1	4.6	5.9
Nano-indentation hardness *H*, GPa	29.7 ± 2.5	29.9 ± 2.5	22.9 ± 2.0	20.5 ± 2.8
Young's modulus *E*, GPa	600 ± 33	434 ± 38	404 ± 21	433 ± 36

2.2 Thermogravimetric differential thermal analysis (TG-DTA), Raman spectroscopy, and XPS (X-ray photoelectron spectroscopy) analysis methods, and tribological property

A thermogravimetric differential thermal analysis device (TG/DTA) was used to conduct heating tests on each coating. The TG/DTA heats the sample while introducing gas and measures the weight difference and differential heat between the sample and a reference material. In this study, the DTG-

60AH (Shimadzu) was used. Each coating deposited on a Si substrate was cut into pieces weighing 8-10 mg and placed into an alumina cell for testing. An empty alumina cell was used as the reference material, and two types of inflow gases, air and dry N_2, were selected. A heating test was conducted from 50°C to 800°C at a rate of 10°C/min.

The atomic percentage of each coating was measured via x-ray photoelectron spectroscopy, (XPS; Ulvac phi Quantera II) with an Al Kα monochromatic x-ray source under vacuum lower than 10^{-5} Pa. Prior to measurements of the topmost surface, Ar ion beam sputter cleaning was performed (acceleration voltage: 4 kV) on an ~2 mm^2 area. Afterward, XPS measurements were performed (acceleration voltage: 15 kV and power: 25 W) on an ~100 μm^2 area. Wide peak measurements for 1 to 1100 eV with 1.0 eV/step were conducted to confirm all elements. In addition, narrow peak measurements for energy ranging from 280.0 to 295.0 eV, and 526.0 to 538.0 eV for C1s, and O1s, respectively, were conducted at 0.1 eV/step. The C1s spectrum was deconvoluted into four peaks corresponding to C-C sp^3, C-C sp^2, C-metal bonds, and a C-O bond, based on the reports by Tokoroyama et al. [40] and Benchikh et al. [42]. The center positions of each peak were 285.3, 284.5, 283.7, and 286.6 eV, respectively, and fitting was performed to set the center positions within a range of ±0.5 eV from these peak positions, with a constant interval between the peaks. After the deconvolution of C1s, we obtained sp^2/sp^3 ratio from the peak area comparison of sp^2 and sp^3. Then, the O1s spectra was deconvoluted into three peaks corresponding to an O-metal bond, an O=C bond, and an O-C bond, based on the reports by Lamour et al. [43], Mukhtar et al. [44]. The peak center positions of each peak were 530.6, 531.4, and 532.1 eV, respectively, and fitting was performed also same procedure of C1s. The O-metal/Peak sum ratio indicates the oxidation ratio between oxygen and metal atoms.

We used Raman spectroscopy comprising an inVia Raman microscope (RENISHAW) with a probe diameter of approximately 2 μm and a 10 mW laser at a 532-nm wavelength covering the range of 800–2000 cm^{-1}. The intensity ratio of the D peak and G peak was obtained from the Raman analysis

results of each coating, and the changes in the carbon structure were clarified [45]. The specimens prepared included the as-deposited sample and those subjected to TG/DTA testing at 800°C in both air and N_2 atmospheres.

The frictional properties of each coating were investigated by a ball-on-disk friction test in air and in O_2. A tungsten carbide (WC) ball with a diameter of approximately 8.0 mm was pressed against a coated disk, which was set on a specimen holder that was connected to a rotary shaft. One sliding cycle comprised a speed of 62.8 mm/s at 23°C under an applied load of 0.3 N. The surface observation was conducted by an optical microscope and a field emission scanning electron microscopy (FE-SEM) with energy dispersive spectroscopy (EDS, Hitachi, SU-8230). The primary electron voltage was 10 kV.

3 Results and discussion

3.1 The thermal proof property of each coating measured by TG/DTA

To clarify the temperature at which the oxidation reaction of each coating begins, changes in the differential thermal analysis were examined using a TG/DTA. The measurement results for each coating in the atmosphere are shown in Fig. 2(a) in air, and (b) in N_2. The temperature was raised from around 50°C at a rate of 10°C per minute, and the temperature difference with the reference material (alumina) was determined from changes in the thermocouple's electromotive force. For each coating, an endothermic reaction, appearing as a convex curve, was observed with the increase in temperature in Fig. 2(a) for all coatings in air condition, and only for ta-C:V coating when it heated in N_2 as shown in Fig. 2(b). The respective endothermic temperatures in air were approximately 550°C and 580°C for the ta-C, about 470°C for the ta-C:V, 610°C for the ta-C:Nb, and 620°C for the ta-C:Ta. On the other hand, only ta-C:V coating showed an endothermic reaction about 680°C in N_2 condition.

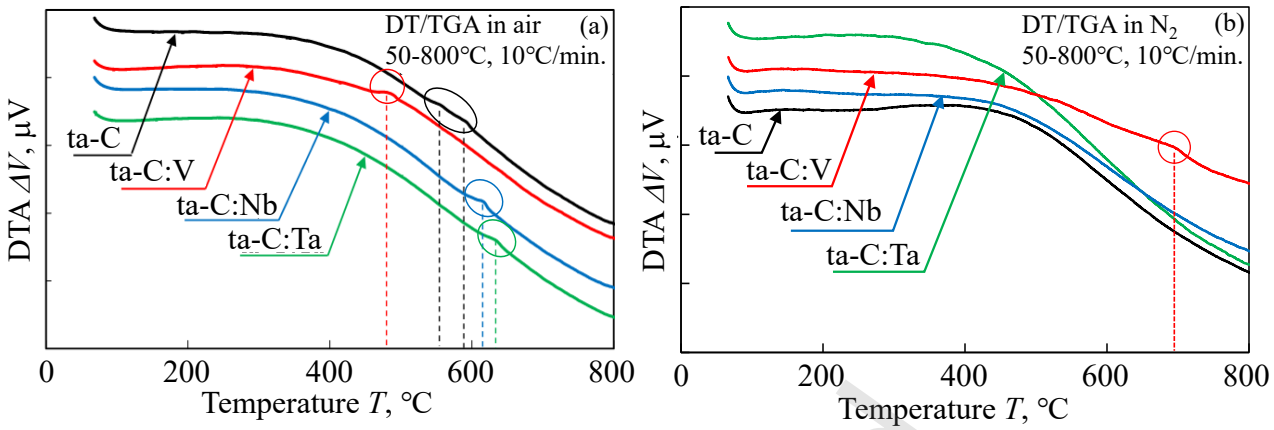

Fig. 2 Endothermic temperature measurement by DTA for each coating, (a) in air, (b) in N_2.

3.2 The optical microscope and SEM/EDS observation for each coating after 800°C heating

The representative results of optical microscope observations of the surface after an 800°C heating experiment using TG/DTA are shown in Fig. 3. Figure 3(a_1) shows the ta-C coating before heating, (a_2) shows the surface after heating in air, and (a_3) shows the surface after heating in N_2. None of the surfaces exhibit characteristic changes due to heating. Next, when Ta and Nb were added in coatings, there were also no characteristic changes, similar to the ta-C coating, so they are not included as figures. On the other hand, ta-C:V showed peeling of the coating or precipitates on the surface after heating. As will be described below, this characteristic surface is vanadium precipitates.

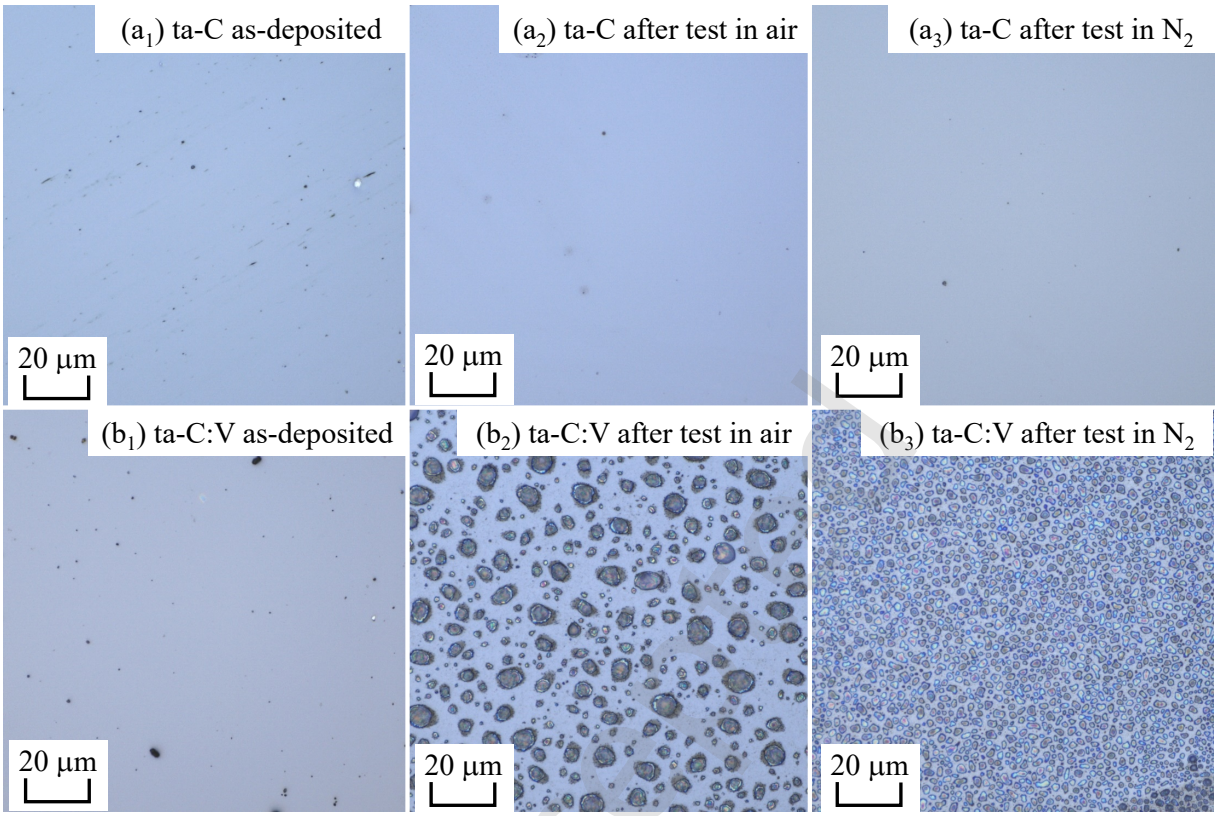

Fig. 3 Optical microscope observation (a_1) as-deposited ta-C, (a_2) after heating test in air, (a_3) after heating test in N_2, (b_1) as-deposited ta-C:V, (b_2) after heating in air, (c1) after heating in N_2.

Optical microscope observations implied vanadium precipitation on the surface, prompting further analysis using SEM/EDS, as shown in Fig. 4. The SEM image of the as-deposited ta-C:V surface is presented in (a_1), with carbon in (a_2), oxygen in (a_3), and vanadium in (a_4). The as-deposited surface shows homogeneous dispersion of vanadium in the coating. The typical surface was observed after heating in air as shown in Fig. 4(b). EDS analysis clearly shows the presence of vanadium and oxygen, highlighted by the white dotted envelope lines. Next, the results of the surface of the specimen heated in N_2 are shown in Fig. 4(c). Similar to the specimen heated in air, deposits believed to be vanadium oxide were observed on the surface. The difference from heating in air is that the size of the deposits is smaller compared to that in air, with a diameter of less than 5 μm. When V was incorporated into the ta-C coating, vanadium was found to precipitate out of the coating upon heating, suggesting the

possibility of a new type of ta-C:V coating in which thermally softened V-oxide precipitates, rather than molten metallic vanadium, act as a lubricious layer.

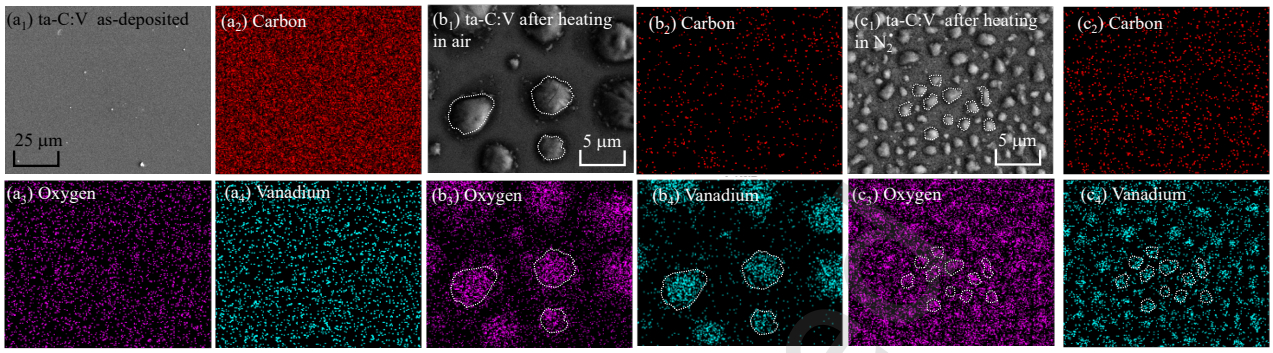

Fig. 4 The SEM and EDS observation results of ta-C:V, (a_1) SEM image of as-deposited, (a_2) carbon, (a_3) oxygen (a_4) vanadium, (b_1) SEM image of after heating in air, (b_2) carbon, (b_3) oxygen, and (b_4) vanadium, (c_1) SEM image of after heating in N_2, (c_2) carbon, (c_3) oxygen, and (c_4) vanadium

3.3 The effect of heating on the carbon structure evaluated using Raman analysis

The results of Raman spectroscopy analysis of each ta-C coating heated up to 400°C and 800°C in air and N_2 atmospheres are shown in Fig. 5. In the test specimens after heating, the intensity of the D peak (around 1330 cm^{-1}) of each coating increased compared to the ta-C coating. Next, when comparing the results of heating in N_2 and air, the ta-C:V coating disappeared after heating to 800°C, and only a peak in the range of 900-1000 cm^{-1}, considered to be from the silicon substrate, was detected in the measurements. The D peak intensity of the ta-C coating slightly increased due to heating in N_2 and air. However, there are few differences between them. The D peak intensity of the Nb and Ta-containing coatings also increased when both coatings heated to 400°C, similar to the ta-C coating. Finally, in the heating test results in air for both ta-C:Ta and ta-C:Nb, no Raman peaks were detected because all coatings had disappeared.

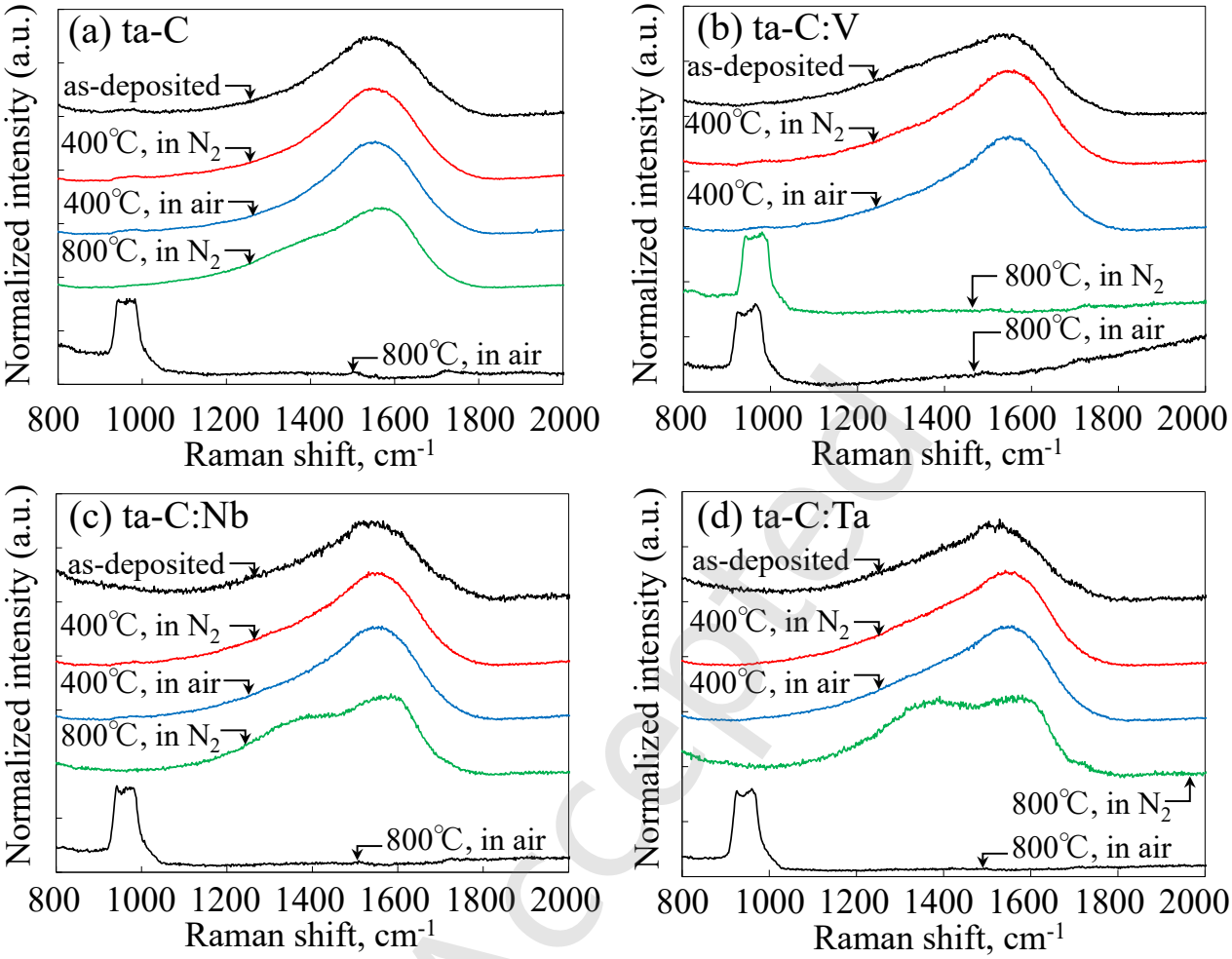

Fig. 5 Raman analysis results, (a) ta-C, (b) ta-C:V, (c) ta-C:Nb, and (d) ta-C:Ta.

The relationship between the I_D/I_G ratio of each coating obtained from Raman measurements and temperature is shown in Fig. 6 for heating in air and nitrogen atmospheres. Firstly, the coatings containing metals (V, Nb, and Ta) show an I_D/I_G ratio of approximately 0.3–0.5 in the as-deposited state. This indicates that the sp^3 -rich carbon matrix is preserved, similar to that in ta-C coatings. Among the specimens heated in air, the I_D/I_G ratio of ta-C and ta-C:V coatings remained unchanged up to 400°C. For the ta-C coating, the I_D/I_G ratio increased under heating conditions at 565°C, and the coating disappeared at 800°C. In contrast, the ta-C:V coating disappeared under heating conditions at 565°C. These results indicate that structural changes involving oxidation of the ta-C and ta-C:V

coatings occur at temperatures above 400°C. On the other hand, the I_D/I_G ratios of ta-C:Nb and ta-C:Ta coatings increased as the temperature was raised from room temperature to 400°C.

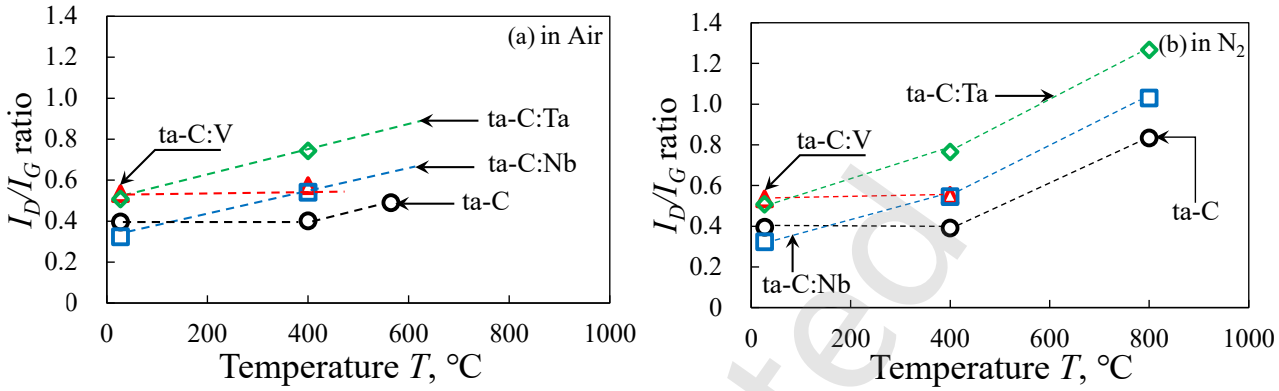

Fig. 6 The relation between heating temperature of coatings and I_D/I_G ratio. (a) heating test in air, and (b) heating test in N_2.

Next, in the results of Raman spectroscopy of specimens heated in a nitrogen atmosphere (Fig. 6(b)), the I_D/I_G ratios of the ta-C and ta-C:V coatings remained unchanged up to 400°C, indicating that no structural changes occurred regardless of the presence of oxygen in the atmosphere. Above 400°C, the ta-C coating underwent structural changes, increasing the I_D/I_G ratio, while the ta-C:V coating disappeared. Meanwhile, the I_D/I_G ratios of the ta-C:Nb and ta-C:Ta coatings showed an increasing trend up to 800°C. This suggests that ta-C coatings containing Nb and Ta are more prone to structural changes with increasing temperature, beyond the oxidation of the carbon framework structure. The structural changes in ta-C coatings containing Ta and Nb due to heating in air from room temperature to 400°C are suggested to result from changes in the carbon framework structure rather than oxidation. However, above 400°C, structural changes due to oxidation reactions and the disappearance of the coating were observed. Regarding the ease of oxidation of each coating, as shown in Fig. 2, the oxidation reaction temperatures were higher for Ta-containing coatings (620°C) and Nb-containing

coatings (610°C) compared to ta-C coatings alone (550 or 580°C). This indicates that the introduction of these elements successfully increased the oxidation reaction temperature.

3.4 Tribological test results for all coatings

The results of the friction tests between each coating and the WC ball are shown in Fig. 7: (a) in air and (b) in an oxygen. In both environments, the final friction coefficient of the ta-C:Ta coating was the lowest, followed by the slightly lower trend of the ta-C:Nb. The friction period up to 1000 cycles is defined as the initial running-in period, and the average value of the friction coefficient from the stable range between 1000 to 2000 cycles is shown in Fig. 8. In air, the ta-C coating showed a friction coefficient of approximately $\mu = 0.094$, while the ta-C:V showed $\mu = 0.11$, the ta-C:Nb showed $\mu = 0.067$, and the ta-C:Ta showed $\mu = 0.043$. In contrast, in the oxygen atmosphere, there was a tendency for the friction coefficients to increase for all coatings except for the ta-C:Ta.

After the friction tests, we measured all coatings for its specific wear rate as shown in Fig. 9. The specific wear rate in air for each coating showed that the ta-C coating was 6.24×10^{-7} mm^3/Nm, while the ta-C:V was higher at 3.8×10^{-6} mm^3/Nm. On the other hand, the ta-C:Nb was 2.2×10^{-6} mm^3/Nm, and the ta-C:Ta was extremely low, at less than 0.3×10^{-7} mm^3/Nm. In an oxygen atmosphere, the wear rate of the ta-C was significantly higher and the coating was also worn out, at 2.1×10^{-5} mm^3/Nm; the ta-C:V was 7.4×10^{-6} mm^3/Nm, the ta-C:Nb was 2.2×10^{-6} mm^3/Nm, and finally, the ta-C:Ta remained very low at 0.8×10^{-7} mm^3/Nm.

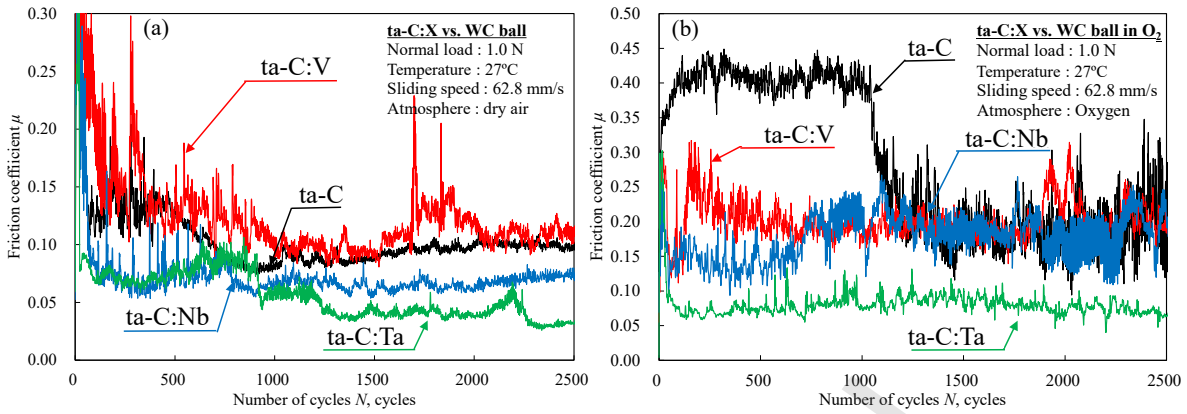

Fig. 7 Friction coefficient as a function of number of sliding cycles, (a) in air, and (b) in N_2.

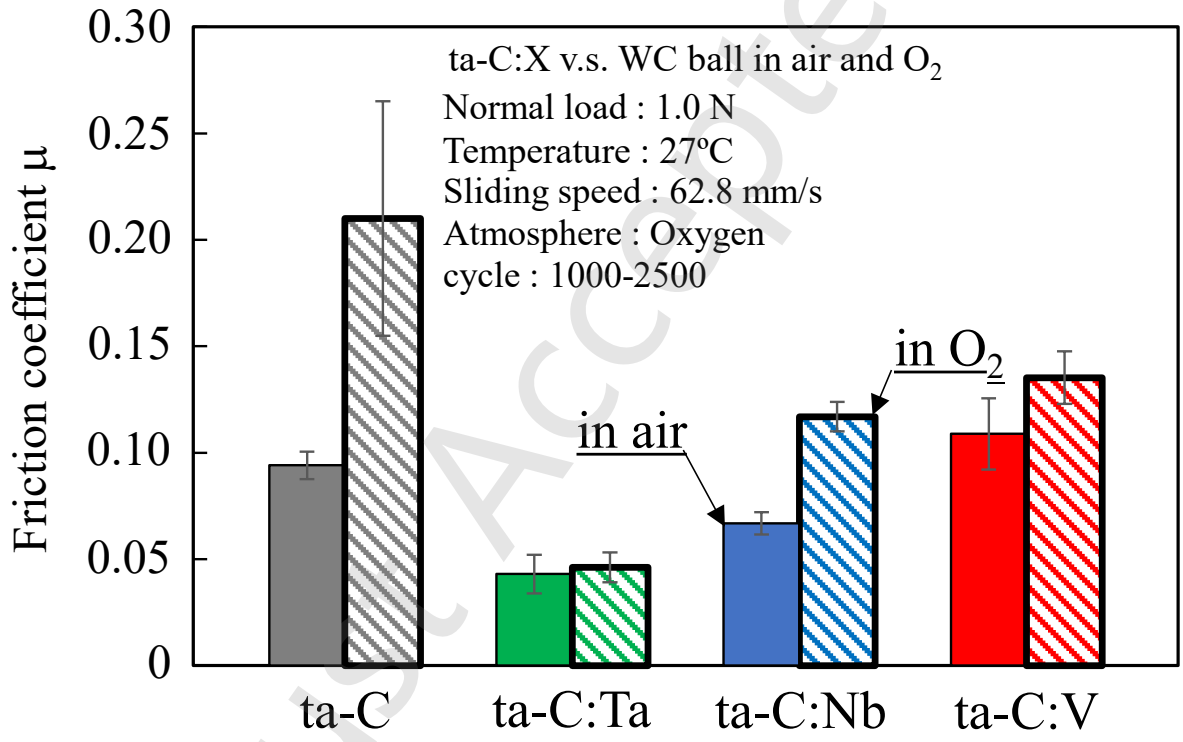

Fig. 8 The average friction coefficient of each coating in air and in N_2.

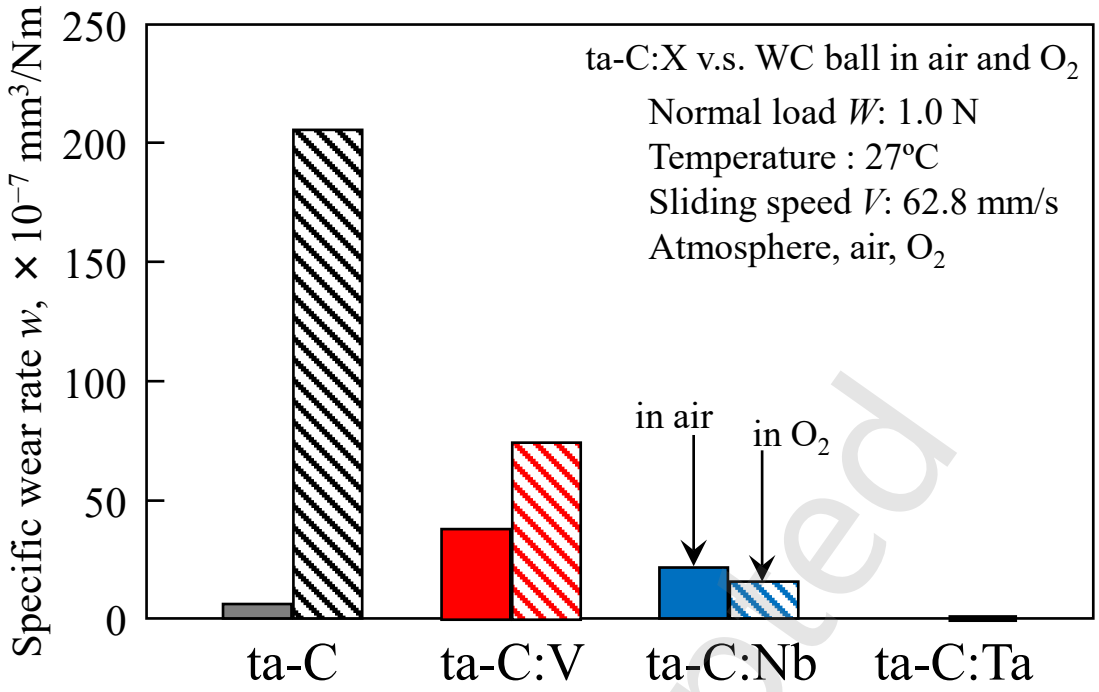

Fig. 9 The specific wear rate of each coating slid in air and in O_2.

3.5 XPS analysis results for all coatings

The XPS analysis results of the wear scars in air and in oxygen for each coating are shown in Fig. 10 (survey data, ta-C was not obtained due to worn out), Fig. 11 (C1s results), and Fig. 12 (O1s results). In the survey measurements, elements detected included Ar (used for surface sputter cleaning), C (comprising the coating), various metal elements, and oxygen. Based on the intensities from the survey data, the atomic percentages (at.%) of elements in the coatings, excluding Ar, were calculated and are presented in Table 2. Before and after friction testing, the oxygen content showed an increasing trend in ta-C and ta-C:V, but a decreasing trend in ta-C:Nb and ta-C:Ta. The C1s peak of carbon was deconvoluted into components corresponding to C-C sp^3 bonds (285.3 eV), C-C sp^2 bonds (284.5 eV), carbon-metal bonds (283.7 eV), and carbon-oxygen bonds (286.6 eV). As shown in Fig. 11 (a1) and (b1), the C-C sp^2, C-C sp^3, and C-O bonds in the ta-C coating exhibited minimal changes before and after friction. For the specimens with added metal elements, C-V, C-Nb, and C-Ta bonds were observed, as shown in Fig. 11 (a_2)–(b_4).

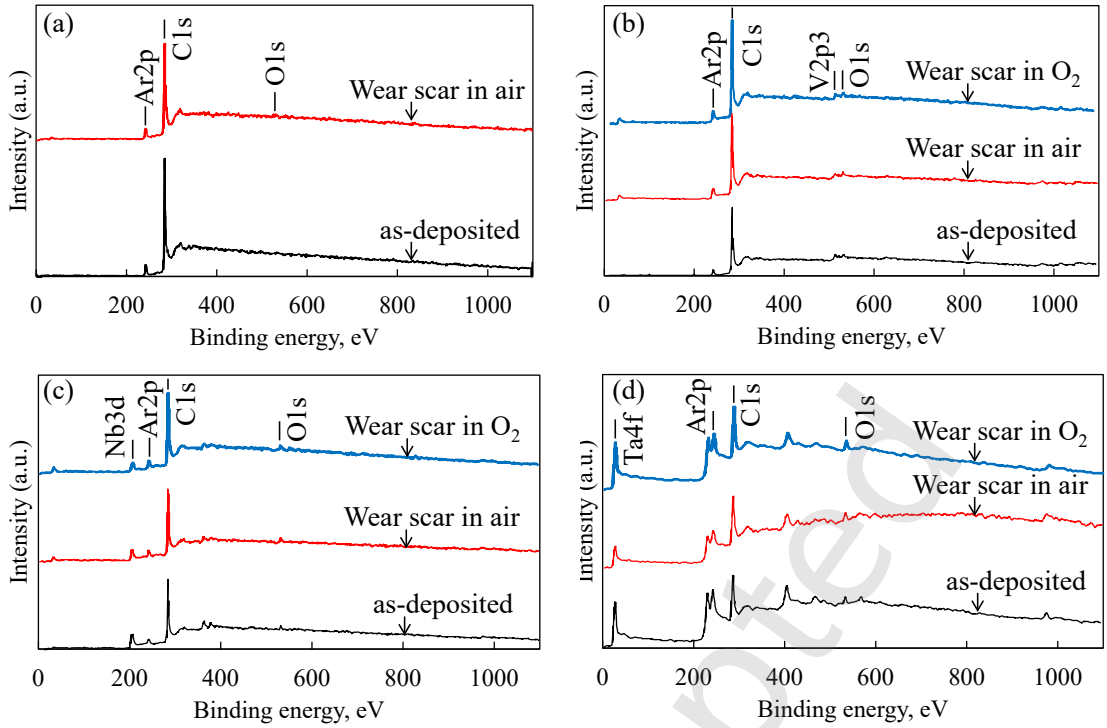

Fig. 10 The XPS analysis results of each coating for survey from 0 to 1100 eV, (a) ta-C, (b) ta-C:V, (c) ta-C:Nb, and (d) ta-C:Ta.

Table 2 The atomic percentages of elements in the coatings.

		C	O	Metal
ta-C	as-deposited	99.04	0.96	-
	Wear scar (in air)	98.57	1.43	-
ta-C:V	as-deposited	95.98	1.54	2.48 (V)
	Wear scar (in air)	96.60	1.82	1.59 (V)
ta-C:Nb	as-deposited	93.45	3.46	3.08 (Nb)
	Wear scar (in air)	95.18	2.73	2.09 (Nb)
ta-C:Ta	as-deposited	86.47	6.43	7.10 (Ta)
	Wear scar (in air)	91.45	4.68	3.88 (Ta)

The O1s peak measurement results are shown in Fig. 12. The low counts in these measurements, along

with fluctuations in the data, suggest that the oxygen content on the surface of each coating was minimal. Despite the low detection intensity, deconvolution of the peaks revealed that, in ta-C coatings, O-C bonds were predominant, as shown in Fig. 12 (a_1) and (b_1). In ta-C:V coatings, as shown in Fig. 12 (a_2) and (b_2), O-V bonds significantly decreased after friction. Meanwhile, in ta-C:Nb coatings (Fig. 12 (a_3) and (b_3)), O-Nb bonds showed little change before and after friction, whereas in ta-C:Ta coatings (Fig. 12 (a_4) and (b_4)), O-Ta bonds exhibited a decrease. Based on these results, the sp^2/sp^3 ratio of the C1s peaks, summarized as Fig. 13(a), and the ratio of O-metal bonds to the total O1s peak intensity, summarized as Fig. 13(b), were analyzed. The sp^2/sp^3 ratio is considered to increase when structural changes in carbon-based hard thin coatings occur due to friction, leading to an increase in the graphite-like structure. For ta-C and ta-C:V coatings, the sp^2/sp^3 ratio showed a decreasing trend, suggesting that their friction coefficient would not decrease. In contrast, ta-C:Nb and ta-C:Ta coatings exhibited an increasing trend in the sp^2/sp^3 ratio. This suggests that the increase in graphite-like structures on the topmost surface of the coatings could lead to reduced shear strength or the realization of incommensurate sliding [31] between graphite layers, resulting in lower friction. The original high-resolution XPS spectra are provided in Supplementary Figs. C and D for clarity.

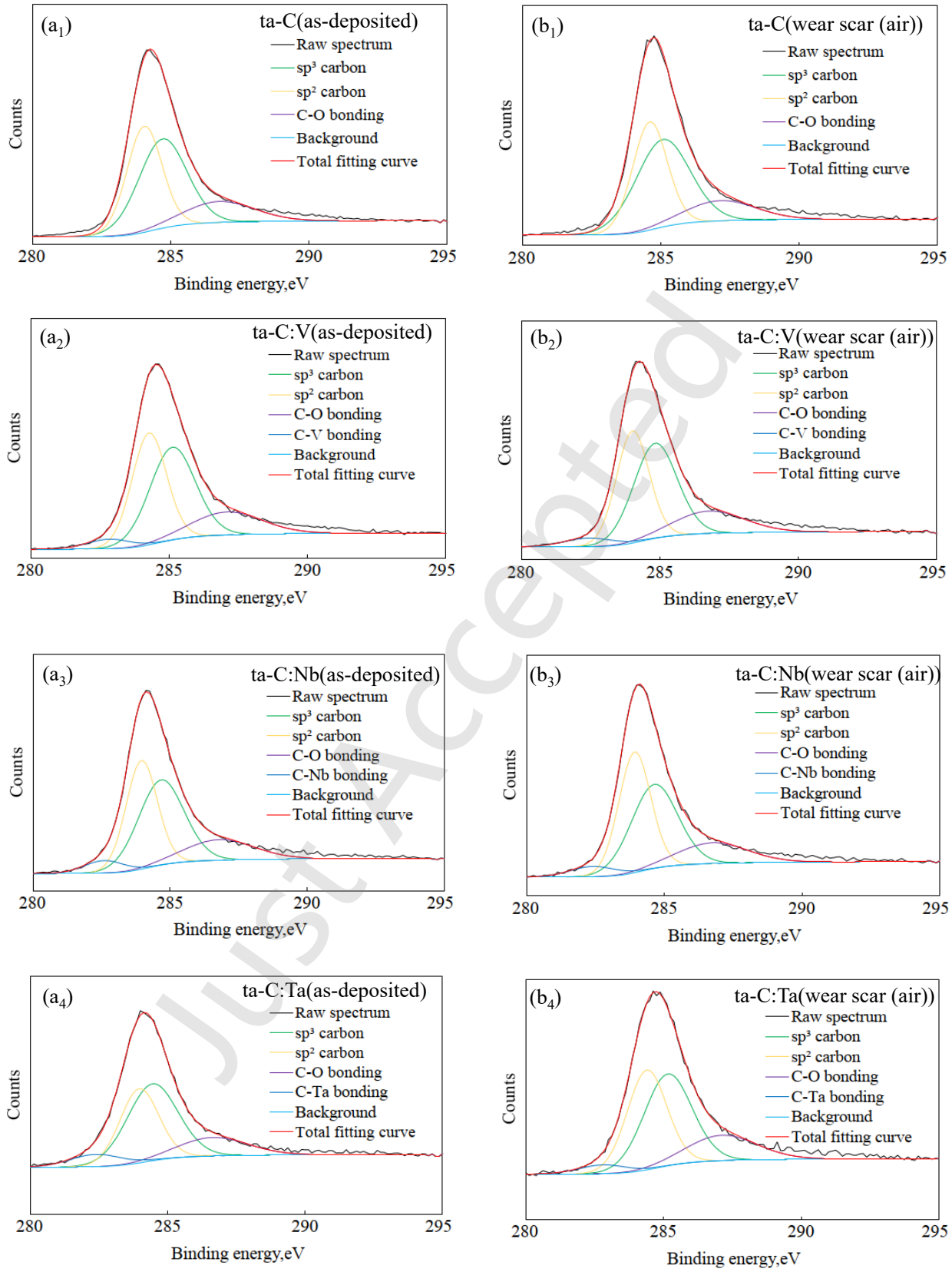

Fig. 11 The XPS narrow analysis for C1s peak, (a_1) as-deposited ta-C, (b_1) wear scar of ta-C in air, (a_2) as-deposited ta-C:V, (b_2) wear scar of ta-C:V in air, (a_3) as-deposited ta-C:Nb, (b_3) wear scar of

ta-C:Nb in air, (a4) as-deposited ta-C:Ta, and (b4) wear scar of ta-C:Ta in air.

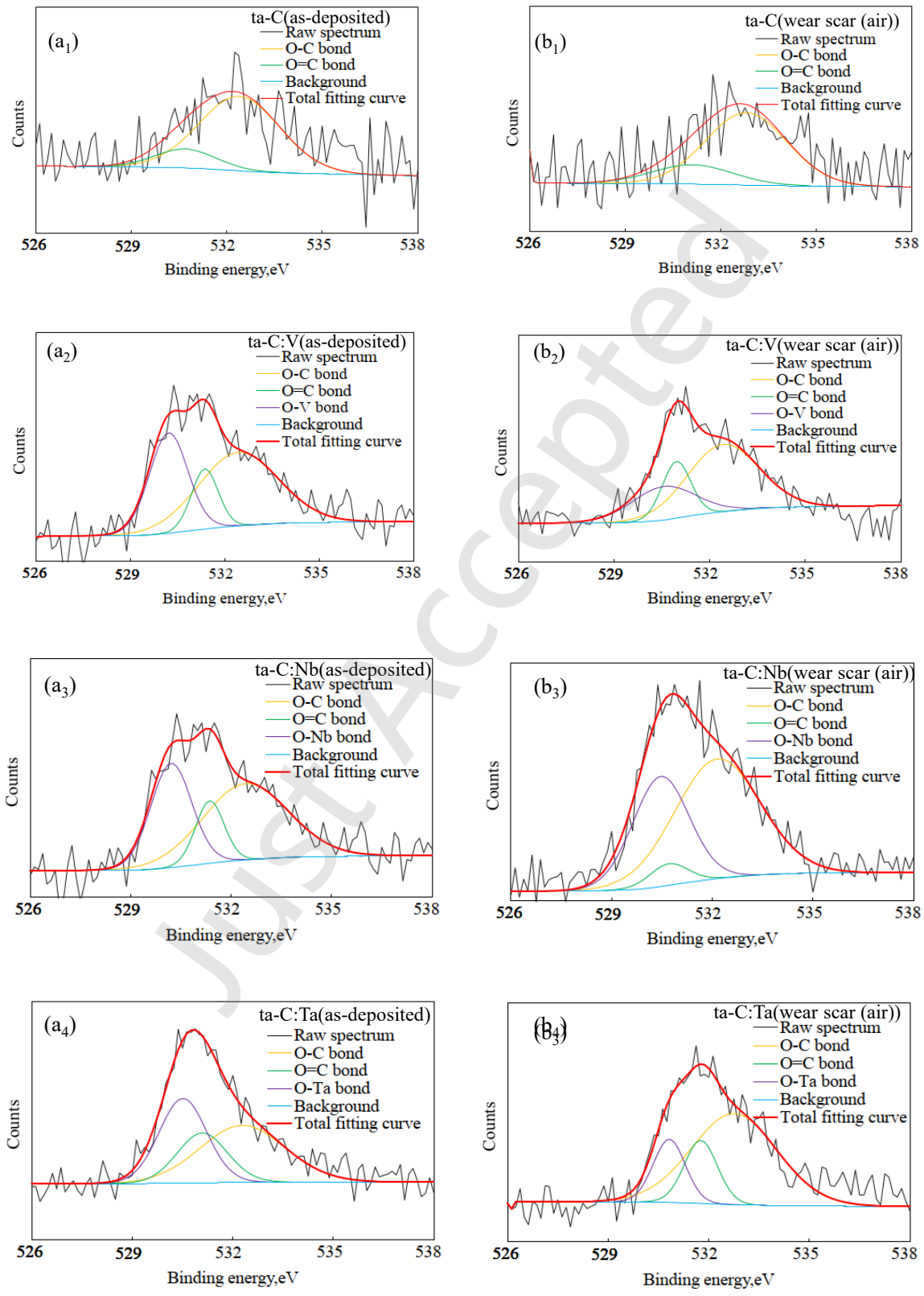

Fig. 12 The XPS narrow analysis for O1s peak, (a_1) as-deposited ta-C, (b_1) wear scar of ta-C in air, (a_2) as-deposited ta-C:V, (b_2) wear scar of ta-C:V in air, (a_3) as-deposited ta-C:Nb, (b_3) wear scar of ta-C:Nb in air, and (a_4) as-deposited ta-C:Ta, (b_4) wear scar of ta-C:Ta in air.

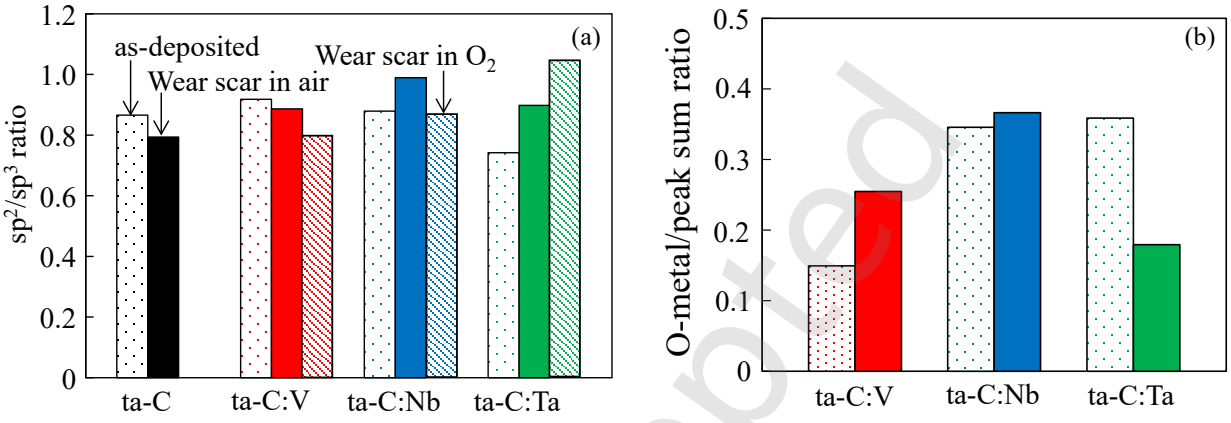

Fig. 13(a) The sp^2/sp^3 ratio of each coating for as-deposited and wear scar in air, and (b) O-metal/peak sum ratio of each element doped coatings.

For the promotion of low friction due to the graphite structure mentioned above, it is necessary for O and metals present in C-O and C-metal bonds within the coating to be expelled from the coating. This would leave behind dangling bonds of carbon atoms, which could then form C-C sp^2 bonds. In the O1s peak data shown in Fig. 12, O-metal bonds within the coatings exhibit little change before and after friction, except in the case of the ta-C:Ta coating. This suggests that the oxidized metal components in the coatings do not change significantly due to friction and likely do not influence the carbon atoms structure governing the entire coating.

On the other hand, C-O bonds directly affect the bonding state of carbon atoms. Therefore, it is essential to quantitatively evaluate the detachment of oxygen bound to carbon atoms. Based on the survey data shown in Fig. 10 and the extracted O/C ratios from Table 2, as well as the sp^2/sp^3 ratios obtained from the C1s spectra, these results are summarized in Fig. 14. For the coatings that exhibited

low friction in air, ta-C:Nb (μ = 0.067) and ta-C:Ta (μ = 0.043), a decrease in the O/C ratio and an increase in the sp^2/sp^3 ratio were observed. In contrast, for ta-C (μ = 0.094) and ta-C:V (μ = 0.11), which did not exhibit a decrease in the friction coefficient, an increase in the O/C ratio and a decrease in the sp^2/sp^3 ratio were observed. These results highlight two distinct trends between the coatings with reduced friction and those without.

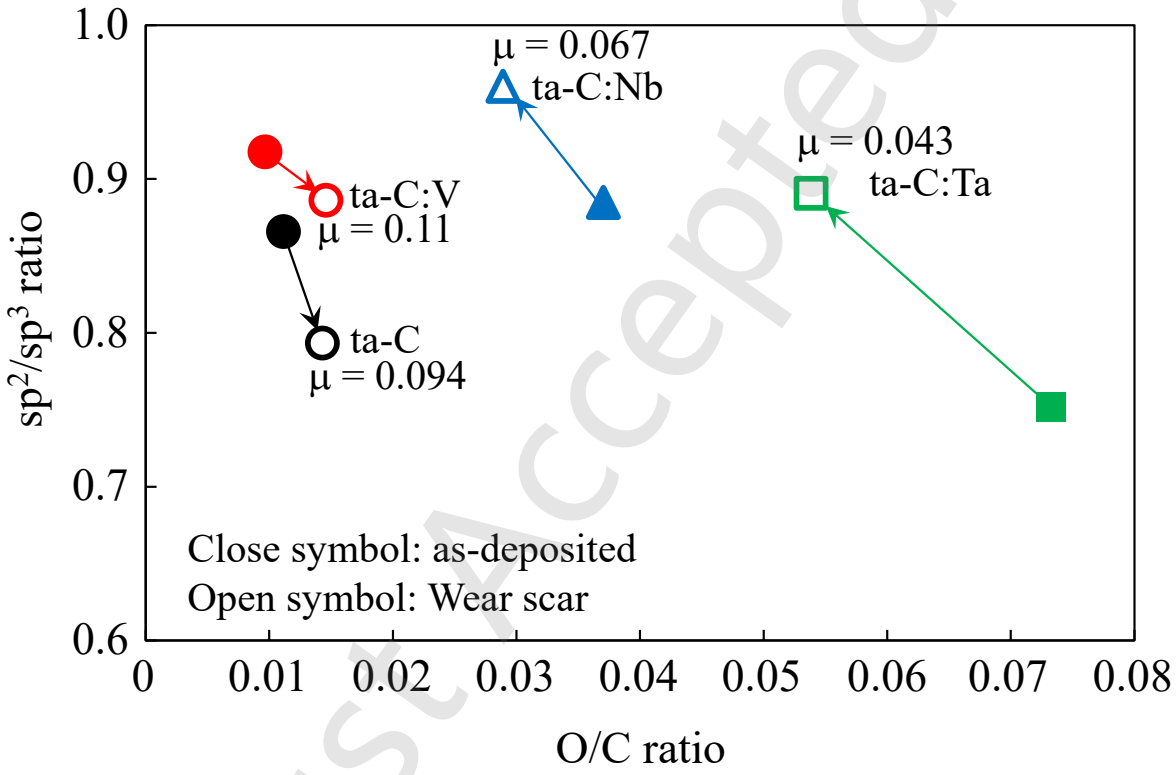

Fig. 14 The relation between O/C ratio of each coating before and after friction and sp^2/sp^3 ratio.

4 Conclusions

In this study, we aimed to improve the oxidation resistance of ta-C caotings by introducing group 5 elements. The coatings were deposited, and their mechanical properties, as well as their thermogravimetric changes in both air and nitrogen, were measured to identify the elements that could enhance oxidation resistance. Additionally, we clarified the structural changes in the coatings due to heat and oxidation, and investigated the impact of oxygen desorption within the coatings on friction

reduction associated with these structural changes. The main conclusions obtained are as follows:

1. As a result of introducing group 5 elements into the ta-C coating to improve oxidation resistance, the endothermic temperature of the ta-C coating increased in the Nb-containing (610°C) and Ta-containing (620°C) coatings compared to the ta-C coating (550–580°C).
2. When Nb and Ta were incorporated into the ta-C caoting, it was found that the carbon structure tended to change more easily to sp^2 with heating, while the ta-C coating and V-containing coatings were less prone to this change.
3. In atmospheric friction tests, the ta-C:Ta coating exhibited the lowest average friction coefficient at 0.043, while the ta-C:Nb caoting had the second lowest at 0.067. When V was included, the friction coefficient did not decrease, and it remained around 0.1, similar to that of the ta-C coating.
4. In coatings where oxygen was incorporated, such as Nb and Ta coatings, oxygen desorbed with friction, causing an increase in sp^2 structure and resulting in a lower friction coefficient. On the other hand, the ta-C and ta-C:V coatings did not show oxygen desorption or an increase in sp^2 structure with friction, which resulted in a higher friction coefficient.

When V was incorporated into the ta-C coating, it was found that the vanadium precipitated out of the coating upon heating. This characteristic suggests the possibility of a new type of ta-C coating, where molten vanadium is precipitated by temperature and acts as a lubricant.

Acknowledgements

Part of this research was conducted with the support of Human resource development and research project on production technology for aerospace industry: Subsidy from Gifu Prefecture, MEXT KAKENHI Grant Number JP23H01327, JST FOREST Program, Grant Number: JPMJFR212E.

Declaration of competing interest

The authors have no competing interests to declare that are relevant to the content of this article.

References

[1] Erdemir A, Eryilmaz OL, Nilufer IB, Fenske GR. Synthesis of superlow-friction carbon films from highly hydrogenated methane plasmas. *Surf Coat Technol* **133–134**:448–454 (2000)

[2] Donnet C, Fontaine J, Grill A, Le Mogne T. The role of hydrogen on the friction mechanism of diamond-like carbon films. *Tribol Let* **9**:137–142 (2001)

[3] Umada N, Kanda K, Niibe M, Hirata Y, Ohtake N, Akasaka H. Oriented sp2 bonded carbon structure of hydrogenated amorphous carbon films. *Diam Relat Mat* **131**:109533 (2023)

[4] Taib MTB, Umehara N, Tokoroyama T, Murashima M, The Effect of UV Irradiation to a-C:H on Friction and Wear Properties under PAO Oil Lubrication Including MoDTC and ZnDTP. *Tribology Online* **13**:119–130 (2018)

[5] Kassim KAM, Tokoroyama T, Murashima M, Umehara N. The Wear Classification of Molybdenum-derived Particles on Silicon and Hydrogenated Diamond-Like Carbon at Room Temperature. *Tribol Int* **147**:106176 (2020)

[6] Aboua KAM, Umehara N, Kousaka H, Tokoroyama T, Murashima M, Mustafa MMB, Mabuchi, Y, Higuchi T, Kawaguchi M. Effect of mating material and graphitization on wear of a-C:H coating in boundary base oil lubrication. *Tribol Let* **68**(24): s11249-019-1248-6 (2020)

[7] Kassim KAM, Tokoroyama T, Murashima M, Lee WY, Umehara N, Mustafa MMB, Wear acceleration of a-C:H coatings by Molybdenum-derived particles: Mixing and temperature. *Tribol Let* **159**:106944 (2021)

[8] Masripan NAB, Ohara K, Umehara N, Kousaka H, Tokoroyama T, Inami S, Zushi K, Fujita M, Hardness effect of DLC on tribological properties for sliding bearing under boundary lubrication condition in additive-free mineral base oil. *Tribol Int* **65**: 265–269 (2013)

[9] Tasdemir HA, Wakayama M, Tokoroyama T, Kousaka H, Umehara N, Mabuchi Y, Higuchi T, Ultra-low friction of tetrahedral amorphous diamond-like carbon (ta-C DLC) under boundary lubrication in poly alpha-olefin (PAO) with additives. *Tribol Int* **65**:286–294 (2013)

[10] Tasdemir HA, Wakayama M, Tokoroyama T, Kousaka H, Umehara N, Mabuchi Y. Higuchi T. Wear behaviour of tetrahedral amorphous diamond-like carbon in additive containing lubricants. *Wear* **307**(1–2):1–9 (2013)

[11] Tasdemir HA, Wakayama M, Tokoroyama T, Kousaka H, Umehara N, Mabuchi Y, Higuchi T. The effect of oil temperature and additive concentration on the wear of non-hydrogenated DLC coating. *Tribol Int* **77**:65–71 (2014)

[12] Mustafa MMB, Umehara N, Tokoroyama T, Murashima M, Shibata A, Utsumi Y, Moriguchi H. Effect of mesh structure of tetrahedral amorphous carbon ta-C coating on friction and wear properties under base-oil lubrication condition. *Tribol Int* **147**:105557 (2020)

[13] Lee WY, Jang YJ, Umehara N, Tokoroyama T, Murashima M, Effect of defects on wear behavior in ta-C coating prepared by filtered cathodic vacuum arc deposition. *Diam Relat Mat* **105**:107789 (2020)

[14] Tokoroyama T, Goto M, Umehara N, Nakamura T, Honda F, Effect of nitrogen atoms desorption on the friction of the CNx coating against Si_3N_4 ball in nitrogen gas. *Tribol Let* **22**(3):215–220 (2006)

[15] Tokoroyama T, Kamiya M, Umehara N, Wang C, Diao DF, Influence of UV irradiation for low friction performance of CNx coatings. *Lubrication Science* **24**:129–139 (2012)

[16] Nishimura H, Umehara N, Kousaka H, Tokoroyama T. Clarification of relationship between friction coefficient and transformed layer of CNx coating by in-situ spectroscopic analysis. *Tribol Int* **93B**:660–665 (2016)

[17] Liu X, Yamaguchi R, Umehara N, Murashima M, Tokoroyama T. Effect of oil temperature and counterpart material on the wear mechanism of ta-CNx coating under base oil lubrication. *Wear* **390–391**:312–321 (2017)

[18] Liu X, Umehara N, Tokoroyama T, Murashima M, Tribological properties of ta-CNx coating sliding against steel and sapphire in unlubricated condition. *Tribol Int* **131**:102–111 (2019)

[19] Tasdemir HA, Tokoroyama T, Kousaka H, Umehara N, Mabuchi Y. Influence of zinc dialkyldithiophosphate tribofilm formation on the tribological performance of self-mated diamond-like carbon contacts under boundary lubrication. *Thin Solid Films* **562**:389–397 (2014)

[20] Aboua KAM, Umehara N, Kousaka H, Tokoroyama T, Murashima M, Tasdemir HA, Mabuchi Y, Higuchi T, Effect of ZnDTP Triboflim's morphology on friction behaviors of DLC coatings: Tribofilm characterization by 3D scanning electron microscope observation. *JAMDSM* **12**(7):JAMDSM0129 (2018)

[21] Aboua KAM, Umehara N, Kousaka H, Tokoroyama T, Murashima M, Mabuchi Y, Higuchi T, Kawaguchi M, Effect of carbon diffusion on friction and wear behaviors of diamond-like carbon coating against Cr-plating in boundary base oil lubrication. *Tribology Online* **13**:290–300 (2018)

[22] Aboua KAM, Umehara N, Kousaka H, Tokoroyama T, Murashima M, Mabuchi M, Higuchi T, Kawaguchi M, Effect of carbon diffusion on friction and wear behaviors of diamond-like carbon coating against germanium in boundary base oil lubrication. *Tribol Let* **67**(2):65 (2019)

[23] Mustafa MMB, Umehara N, Tokoroyama T, Murashima M, Shibata A, Utsumi Y, Moriguchi H, Effect of pillar and mesh structure of tetrahedral amorphous carbon ta-C coatings on the wear properties and fracture toughness of the coating. Tribology Online **14**(5):388–397 (2019)

[24] Hashizume N, Murashima M, Umehara N, Tokoroyama T, Lee WY, In situ observation of the formation of MoDTC-derived tribofilm on a ta-C coating using reflectance spectroscopy and its effects on friction. *Tribol Int* **162**:107128 (2021)

[25] Kim JI, Lee WY, Tokoroyama T, Murashima M, Umehara N, Friction characteristics of amorphous carbon coating against various 3d-transition metals. *Tribol Int* **174**:107690 (2022)

[26] Kim JI, Lee WY, Tokoroyama T, Murashima M, Umehara N, Tribo-chemical wear of various 3d-transition metals against DLC: Influence of tribo-oxidation and low-shear transferred layer. *Tribol Int* **177**:107938 (2023)

[27] Lee WY, Tokoroyama T, Jang YJ, Umehara N. Investigating running-in behavior to understand wear behavior of ta-C coating with filtered cathodic vacuum arc deposition. *Journal of Tribologi* **23**:38–47 (2019)

[28] Murashima M, Oyama S, Kousaka H, Tokoroyama T, Lee WY, Umehara N, New in situ low-friction technology for diamond-like carbon coatings using surface discharge treatment in ambient air. *Tribol Int* **165**:107306 (2021)

[29] Lee WY, Tokoroyama T, Murashima M, Umehara N, Horaguchi N, Ishimoto T. Realization of near-less friction of ta-CNx coating under R32 refrigerant environment. *Tribol Int* **168**:107404 (2022)

[30] Wu W, Murashima M, Saso T, Tokoroyama T, Lee WY, Kousaka H, Umehara N. New in situ superlow-friction method for nitrogen-containing diamond-like carbon coatings using dielectric barrier discharge treatment in ambient air. *Tribol Int* **174**:107749 (2022)

[31] Dienwiebel M, Verhoeven GS, Pradeep N, Frenken JWM, Heimberg JA, Zandbergen HW. Superlubricity of graphite. Phys Rev Let **92**(12):126101 (2004)

[32] Tokoroyama T, Fujiwara C, Murashima M, Yamaguchi M, Umehara N. Effect of the graphite domain direction on the friction coefficient of tetrahedral amorphous carbon nitride. *Diam Relat Mat* **143**:110853 (2024)

[33] Yamada N, Watari T, Takeno T, Adachi K, Effect of Oxygen on the Self-formation of Carbonaceous Tribolayer with Carbon Nitride Coatings under a Nitrogen Atmosphere. *Tribol Let* **65**(27):s11249-016-0809-1 (2017)

[34] Kim JI, Lee WY, Tokoroyama T, Umehara N. Superlubricity with Graphitization in Ti-doped DLC/Steel Tribopair: Response on Humidity and Tempereture. *Applied Mat Int* **15**:19715–19729 (2023)

[35] Jang YJ, Kim JI, Kim WS, Kim DH, Kim JK. Thermal stability of Si/SiC/ta-C composite coatings and improvement of tribological properties through high-temperature annealing. Scientific Reports **12**:3536 (2022)

[36] Bi J, Yang M, Peng J, Sheng R, Li L, Yick ML. Effect of Si/O doping on the thermal stability of non-bonded hydrogenated diamondlike carbon coatings, *Surf Coat Technol* **374**: 1006-1014 (2019)

[37] Kim JY, Magyari-Kope B, Nishi Y, Ahn JH. First-principles study of carbon impurity effects in the pseudo-hexagonal Ta_2O_5. *Curr Applied Phys* **16**:638–643 (2016)

[38] Nyberg H, Tokoroyama T, Wiklund U, Jacobson S, Design of low-friction PVD coating systems with enhanced running-in performance – Carbon overcoats on TaC/aC. *Surf Coat Technol* **222**:48–54 (2013)

[39] Tokoroyama T, Hattori T, Umehara N, Kousaka H, Manabe K, Kishi M, Fuwa Y, Ultra-low friction properties of carbon nitride tantalum coatings in the atmosphere. *Tribol Int* **103**:388–393 (2016)

[40] Tokoroyama T, Tagami Y, Murashima M, Umehara N, Kousaka H. Tribological property of ta-CNx:Ta deposited via ion beam assisted-filtered arc deposition. *Tribol Int* **168**:107450 (2022)

[41] Lee WY, Tokoroyama T, Jang YJ, Umehara N. Effect of substrate bias and temperature on friction and wear properties for ta-C coating prepared under different substrate bias voltages with filtered cathodic vacuum arc deposition. *Tribology Online* **13**(5):241–247 (2018)

[42] Benchikh N, Garrelie F, Wolski K, Donnet C, Fillit RY, Rogemond F, Subtil JL, Rouzaud JN, Laval JY. Nanocomposite tantalum-carbon-cased films deposited by femtosecond pulsed laser ablation. *Thin Solid Films* **494**(1–2):98–104 (2006)

[43] Lamour P, Fioux P, Ponche A, Nardin M, Vallat MF, Dugay P, Brun JP, Moreaud N, Pinvidic JM. Direct measurement of the nitrogen content by XPS in self-passivated TaNx thin films. *Surf Int Analy* **40**(11):1430–1437 (2008)

[44] Ahmed M, Anthony Byrne J, McLaughlin JAD. Glycine Adsorption onto DLC and N-DLC Thin Films Studied by XPS and AFM. *e-J Surf Sci Nano* **7**:217–224 (2009)

[45] Ferrari AC, Robertson J, Interpretation of Raman spectra of disordered and amorphous carbon. *Phys Rev B. Part B* **61**:14095 (2000)

Takayuki Tokoroyama is Associate Professor in Micro-Nano Mechanical Science and Engineering at Nagoya University, Japan. He serves as Principal Investigator of the JST FOREST Program and is involved in various collaborative research projects. He received his academic training at Tokyo Metropolitan Institute of Technology and Nagoya Institute of Technology. He has authored more than 130 publications in peer-reviewed journals and over 200 papers in international conference proceedings. His research interests include hard carbon coatings, ion beam techniques, tribology and medical-engineering collaboration. He is internationally recognized and frequently invited as a speaker. He also serves as a reviewer and is a technical committee for tribology member of IFToMM.